Obrabotka metallov (tekhnologiya, oborudovanie, instrumenty) = Metal Working and Material Science. 2025 vol. 27 no. 4 pp. 80–95
ISSN: 1994-6309 (print) / 2541-819X (online)
DOI: 10.17212/1994-6309-2025-27.4-80-95

NSTU NETI

Obrabotka metallov - Metal Working and Material Science

Journal homepage: http://journals.nstu.ru/obrabotka_metallov

Mathematical analysis of the titanium alloy surface profile under various modes of electromechanical treatment

Mikhail Romanenko [1, a, *] , ***Igor Zakharov*** [1, b], ***Vyacheslav Bagmutov*** [1, c], ***Vladislav Barinov*** [1, d], ***Minh Tuong Nguyen*** [2, e]

[1] Volgograd State Technical University, 28 Lenin Avenue, Volgograd, 400005, Russian Federation
[2] Russian Technological University MIREA, 78 Vernadsky Avenue, Moscow, 119454, Russian Federation

[a] https://orcid.org/0000-0002-4800-7151, romanenko.mihail2009@yandex.ru; [b] https://orcid.org/0000-0001-7177-7245, 4zaxap@gmail.com;
[c] https://orcid.org/0000-0003-3648-8450, sopromat@vstu.ru; [d] https://orcid.org/0000-0001-9400-7366, barinov@vstu.ru;
[e] https://orcid.org/0009-0004-7484-7009, nguen_m@mirea.ru

ARTICLE INFO

Article history:
Received: 29 May 2025
Revised: 30 June 2025
Accepted: 10 October 2025
Available online: 15 December 2025

Keywords:
Profilogram
Microgeometry
Fast *Fourier* transformation (*FFT*)
Harmonic
Electromechanical treatment
Surface plastic deformation
Titanium alloy *VT22*

Funding
The study was carried out with financial support from the Russian Science Foundation (project No. 25-29-20241).

ABSTRACT

Introduction. Currently, many mathematical approaches exist for approximating surface profile curves. Most employ volumetric mathematical expressions to describe surface profile parameters after various types of processing. **Purpose of the work** is to select a mathematical apparatus that is simple enough from an engineering perspective to approximate the surface profile of *VT22* titanium alloy samples after surface plastic deformation (*SPD*) and various electromechanical processing (*EMP*) modes, with the possibility of eliminating random technological errors. **The paper investigates** the effect of *EMP* modes using alternating and direct current at densities of 100, 300, and 600 A/mm^2, considering both the application of force by the deforming tool-electrode (150 N) and its absence (10 N), on the surface geometry of *VT22* titanium alloy samples. The electromechanical processing of metal alloys used in this work can significantly change the geometric profile, structure, and operational properties of the surface. Its distinctive feature is the creation of both microdeviations (roughness) and macrodeviations and relief (waviness, "oil pockets", build-ups from metal surfacing to the repair size) on the surface. **Research methods.** Profilometric analysis was performed using a *PM-7* device, followed by processing of the roughness measurement results using the fast *Fourier* transform (*FFT*) on the surface of a cylindrical sample made of *VT22* titanium alloy with a diameter of 16 mm after electromechanical rolling with an tool-electrode, previously subjected to semi-finish turning. The error of the model curves of the surface profile was estimated using the *Pearson* correlation coefficient (***R***). **Results and discussion.** The use of high-density direct current helps to obtain a surface with a high relative support length of the profile (98.8%), a low arithmetic mean deviation of the profile (1.9 μm), and an average step of profile irregularities (56 μm). Based on the *FFT*, the considered modes of electromechanical processing contribute to the formation of profile waviness with different pitch and height. The greatest correlation is observed for modes 2, 4, and 9 ($R > 0.7$), while the lowest correlation coefficient was noted for *EMP* with a direct current density of 100 and 300 A/mm^2 (modes 5 and 6, $R < 0.25$).

For citation: Romanenko M.D., Zakharov I.N., Bagmutov V.P., Barinov V.V., Nguyen M.T. Mathematical analysis of the titanium alloy surface profile under various modes of electromechanical treatment. *Obrabotka metallov (tekhnologiya, oborudovanie, instrumenty) = Metal Working and Material Science*, 2025, vol. 27, no. 4, pp. 80–95. DOI: 10.17212/1994-6309-2025-27.4-80-95. (In Russian).

Introduction

The ability to control the macro- and microgeometry of metal alloy surfaces following various processing methods is a critical objective throughout the entire lifecycle of machine components in mechanical engineering – from manufacturing and assembly to operation, such as ensuring durable contact interaction between surfaces.

*** Corresponding author**
Romanenko Mikhail D., Ph.D. (Engineering), Senior Lecturer
Volgograd State Technical University,
28 Lenin Avenue,
400005, Volgograd, Russian Federation
Tel.: +7 977 064-06-19, **e-mail:** romanenko.mihail2009@yandex.ru

The theory of technological inheritance plays a significant role in mechanical engineering in forming the required quality of a part's surface layer. In manufacturing, to achieve a specified set of surface properties, all operations and their respective technological stages are taken into account. Quantitative assessment typically employs empirical coefficients of inheritance, which include factors for their mutual influence [1–3].

High-energy surface treatment of metal alloys induces significant restructuring of the crystal lattice and microstructure, alters the stress-strain state, and modifies surface geometry [4–6]. For instance, electromechanical processing (*EMP*) using alternating current on steel alloys can reduce the arithmetic mean deviation of the profile (R_a) to 0.2–0.63 μm in a smoothing mode with a moving tool (roller). Using direct current can reduce Ra by a factor of 2–3 compared to the preceding value [7]. Direct current application, compared to alternating current, enables a higher degree of micro-roughness smoothing (eliminating "noise") [8]. According to [9–14], several surface hardening technologies can substantially improve surface micro-geometry parameters, for example, through high-speed plastic deformation (ultrasonic treatment [12–13]), local melting (laser treatment [13–14]), and positively impact the static and fatigue strength of metal alloys.

Applying mathematical models and methods allows for a detailed analysis of component surface profiles, identifying patterns in their geometry formation, and assessing the contribution of each technological operation to the final quality [15–22].

Most publications utilize combined models based on contact mechanics and fractal theory [15, 16], the geometry of hardening/cutting tools and *Hertz* theory [17, 18], regression and statistical models (linear and stepwise regression, pairwise correlation matrix, particle swarm optimization), discrete *Fourier* transform, and machine learning [19–22].

The purpose of this work is to determine the principal components of the surface profile geometry and to identify the patterns of microgeometry formation on a *VT22* alloy sample subjected to various electromechanical processing (*EMP*) modes using mathematical processing of discrete signal data (fast *Fourier* transform).

To achieve this purpose, the following ***research tasks*** were defined:

1) Prepare a sample from *VT22* titanium alloy and strengthen it according to specified processing modes.

2) Obtain surface profiles and key roughness parameters using an "*ABRIS PM7*" profilograph-profilometer.

3) Perform *FFT* analysis to obtain the main harmonics of the surface profile for each processing mode.

4) Construct model curves of the surface profile for each mode.

5) Classify the model curves and their harmonics according to the type of longitudinal surface profile deviation.

6) Use the correlation coefficient to identify the electromechanical processing (*EMP*) and surface plastic deformation (*SPD*) modes that most accurately represent the surface profile of the sample.

Methods

Cylindrical sample preparation through turning (final diameter 16 mm) and subsequent electromechanical processing (*EMP*) was performed on a *16K20* lathe (Fig. 1). Machining was conducted at a minimum feed rate of 0.125 mm/rev, with two sequential passes removing a 0.2 mm layer from the diameter.

The process of setting up and adjusting the devices for electromechanical treatment is described as follows.

The titanium sample (**1**) is secured in the chuck jaws (**2**). The tailstock quill (**3**) with the current collection unit (**4**) and a centering cone is advanced toward the sample (**1**).

The spring-loaded *EMP* device (**6**) is clamped with the bolts of the tool holder (5) through current-insulating gaskets. The tool-electrode (**7**) is manually brought into contact with the sample with the required force (calibrated via the device's spring).

The coolant supply tube (**8**) is attached to the tool holder (**5**), and power cables with terminals (**9**) are connected to the current collection unit (**4**) and the *EMP* device (**6**). A coolant collection container (**10**) is positioned beneath the processing zone.

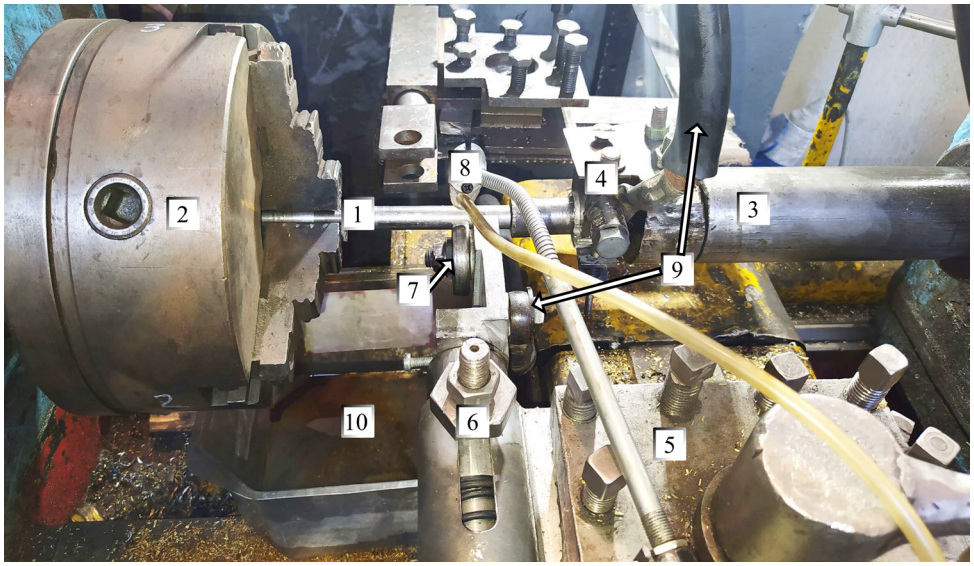

Fig. 1. Schematic of the experimental device for conducting *EMP* on a *16K20* lathe. Key components:

1 – titanium workpiece; 2 – chuck; 3 – tailstock quill; 4 – current collection device; 5 – toolholder; 6 – device for *EMP*; 7 – tool-electrode (roller); 8 – coolant supply tube; 9 – power cables with tips; 10 – container

Electromechanical processing involves passing a high-density electric current through the small contact area between the working tool and the part surface (Fig. 2), with continuous coolant (technical water) supply. This process is characterized by: high local heating and cooling rates (10^5–10^6 °C/c), high current density (up to 1,500 A/mm²), and low voltage (2–6 V). Coolants used include machine oil, specialized emulsions (as in turning/milling), and technical water for achieving hardened microstructures [23].

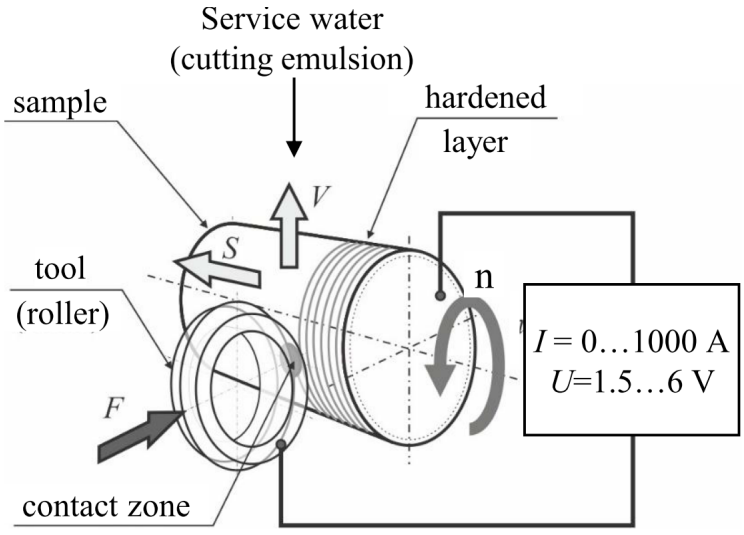

Fig. 2. Schematic of electromechanical processing

Constant parameters for both alternating current (*AC*) and direct current (*DC*) *EMP* were: Longitudinal feed (0.4 mm/rev), rotating frequency (13 rpm).

The tool-electrode was a toroidal roller made of *VK6C* hard alloy (94% *WC*, 6% *Co*) with a 60 mm diameter and a 5–6 mm profile radius. Variable mode parameters are summarized in Table 1.

For all modes, the initial surface was the semi-finish turned surface. Higher initial roughness does not qualitatively improve with additional *EMP* passes [23]. Current densities exceeding 600 A/mm² (regardless of type) were excluded as they caused surface burning and cavity formation. Low current density *EMP*

Table 1

Electromechanical treatment modes with alternating and direct current

Mode No. / Parameters of *EMP*	1	2	3	4	5	6	7	8	9	10
Current density, A/mm²	–	–	$\overline{600}$	$\widetilde{600}$	$\overline{100}$	$\overline{300}$	$\overline{600}$	$\widetilde{100}$	$\widetilde{300}$	$\widetilde{600}$
Tool pressing force, N	–	150	10	10	150	150	150	150	150	150

Note: mode 1 represents the initial state after turning. The symbol "~" denotes alternating current, "–" denotes direct current.

(100 A/mm²) is recommended for surface smoothing without altering microstructure or hardness [23]. Tool-electrode forces below 10 N were deemed impractical, as they prevented reliable contact and led to micro-arcing.

Surface roughness parameters were measured five times per processing mode using an *ABRIS PM-7* profilometer-profilograph.

The fast *Fourier* transform (*FFT*) was employed to determine the duration of periods and amplitude-phase characteristics of height and step irregularities. This method decomposes the original discrete profile signal into a series of harmonic (spectral) components – sinusoids defined by amplitude, phase, and frequency, ordered by magnitude [24].

For constructing predictive models, a general equation (1) describes the dynamics of the studied parameter.

When constructing predictive models of various quantities, a general equation (1) is used to determine the dynamics of the studied quantity: $D(t)$

$$D(t) = T(t) + C(t) + R(t), \tag{1}$$

where $T(t)$ is the main trend; $C(t)$ is the cyclical component; $R(t)$ is the random component ("noise").

The primary equation (2) for constructing the time series $\boldsymbol{y_t}$, incorporating harmonics identified via *FFT*, is:

$$S(t) = \frac{a_0}{2} + \sum_{i=1}^{n}\left(a_i \cos\frac{2\pi}{T_i}t + b_i \sin\frac{2\pi}{T_i}t\right) = \frac{a_0}{2} + \sum_{i=1}^{n} c_i \sin\left(\frac{2\pi}{T_i}t + \varphi_i\right), \tag{2}$$

where a_0 is the constant component (zero harmonic); $c_i = \sqrt{a_i^2 + b_i^2}$ is the amplitude of the $\boldsymbol{i}$-type harmonic; $T_i = N / i$ is the period of the $\boldsymbol{i}$-type harmonic oscillation; N is the number of original data in the time series; a_i, b_i are the *Fourier* time series coefficients [24].

FFT and graph construction were performed in *Microsoft Excel*. The analyzed data series was limited to 2,048 points due to the *FFT* requirement for data length to be a power of two (2^{11} = 2,048). Subharmonics were selected based on *Pearson's* correlation coefficient, maximizing its value for each specific case – a method aligned with prior work [25]. A maximum of five harmonics were used in the equations describing the time series.

Following established literature [26], macro- and micro-deviations of a part's longitudinal surface profile are classified by the ratio of the step length to the height of the protrusion ($\boldsymbol{l}/\boldsymbol{H}$):

Macro-deviation: $\boldsymbol{l}/\boldsymbol{H} \geq 1{,}000$

Waviness: $50 \leq \boldsymbol{l}/\boldsymbol{H} \leq 1{,}000$

Roughness: $0 \leq \boldsymbol{l}/\boldsymbol{H} \leq 50$

A diagram illustrating these scale levels of longitudinal profile deviations is shown in Fig. 3. These ratios were used to classify the model curves by their deviation scale.

A diagram explaining the difference in scale levels of profile deviations of longitudinal sections is presented in Fig. 3.

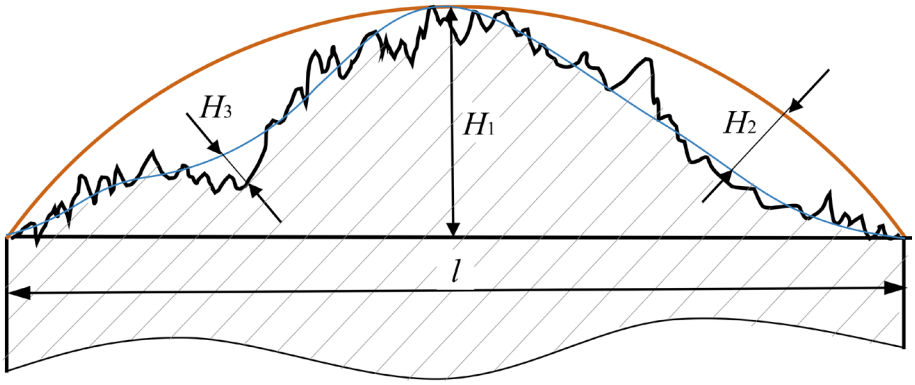

Fig. 3. Scheme of differentiation of surface quality parameters of parts:

H_1 – shape deviation (barrel shape), H_2 – surface waviness (second-order shape deviation), H_3 – surface roughness (third-order shape deviation, microroughness), l – base length

These ratios were used to classify the model curves by their deviation scale.

Results and Discussion

Electromechanical processing (*EMP*) of a *VT22* titanium alloy sample under eight distinct modes yielded surfaces with varied macro- and micro-geometric parameters and discoloration (Fig. 4).

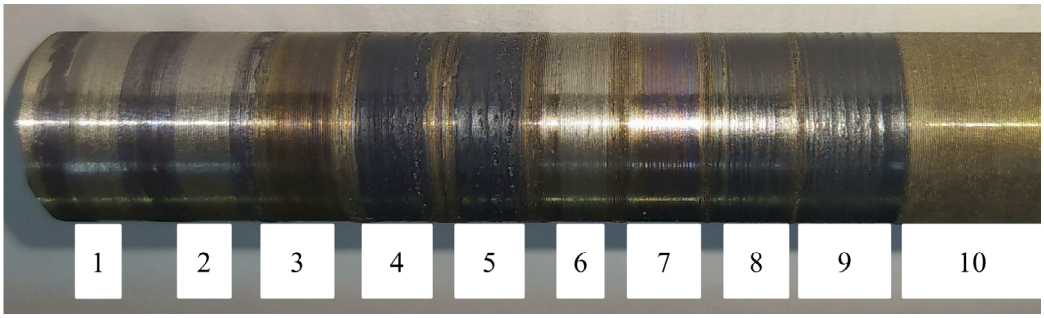

Fig. 4. Micrographs showing the surface morphology of *VT22* titanium alloy sample following different electromechanical processing (*EMP*) modes. Modes:

1 – 150 N; 2 – $\widetilde{100}$ A/mm^2, 150 N; 3 – $\widetilde{300}$ A/mm^2, 150 N; 4 – $\widetilde{600}$ A/mm^2, 10 N; 5 – $\widetilde{600}$ A/mm^2, 150 N; 6 – $\overline{100}$ A/mm^2, 150 N; 7 – $\overline{300}$ A/mm^2, 150 N; 8 – $\overline{600}$ A/mm^2, 10 N; 9 – $\overline{600}$ A/mm^2, 150 N; 10 – initial (conventional turning, feed: 0.125 mm/rev)

The reference state was the initial surface after semi-finish turning, with the following roughness parameters: $\boldsymbol{R_a}$ = 12.42 μm; $\boldsymbol{S_m}$ = 128 μm; $\boldsymbol{t_{60}}$ (60%) = 44.7%. The section level of the profile's support length was chosen to be 60%. The arithmetic mean deviation of the profile ($\boldsymbol{R_a}$) was used as the primary height parameter due to its informativeness. Surface processing analysis revealed that modes No. 3, 7, and 9 were optimal in terms of height, step, and structural surface layer parameters (Fig. 5).

The mode of electromechanical smoothing (*EMS*) with high-density direct current (600 A/mm^2, **Mode 3**) reduced the indicators: $\boldsymbol{R_a}$ by a factor of 6.52, $\boldsymbol{S_m}$ by a factor of 1.27, and $\boldsymbol{t_{60}}$ increased by a factor of 2.21.

EMP with direct current of the same density with a pressing force of 150 N (**Mode 7**) reduced $\boldsymbol{R_a}$, $\boldsymbol{S_m}$ by factors of 4.43 and 2.28, respectively, and practically doubled the $\boldsymbol{t_{60}}$.

Alternating current with a density of 600 A/mm^2 during *EMP* (**Mode 10**) resulted in the appearance of secondary roughness due to the higher amplitude of AC compared to **Mode 9** [8], while the step parameter ($\boldsymbol{S_m}$) for these modes decreased by 6%, and the $\boldsymbol{t_{60}}$ parameter increased by 1.58 times (Fig. 5).

Rolling without current (**Mode 2**) and *EMS* with low current density (100 A/mm²) using either *AC* (**Mode 5**) or *DC* (**Mode 8**) did not qualitatively alter the surface profile (Fig. 5).

Despite the low processing speed and low deformation force (10 N) in **Modes 3** and **4**, R_a decreased significantly (to 1.9 μm) and t_{60} increased to 98.8% (Figs. 5 and 6, **Mode 3**), a similar effect was observed in the prior research [27].

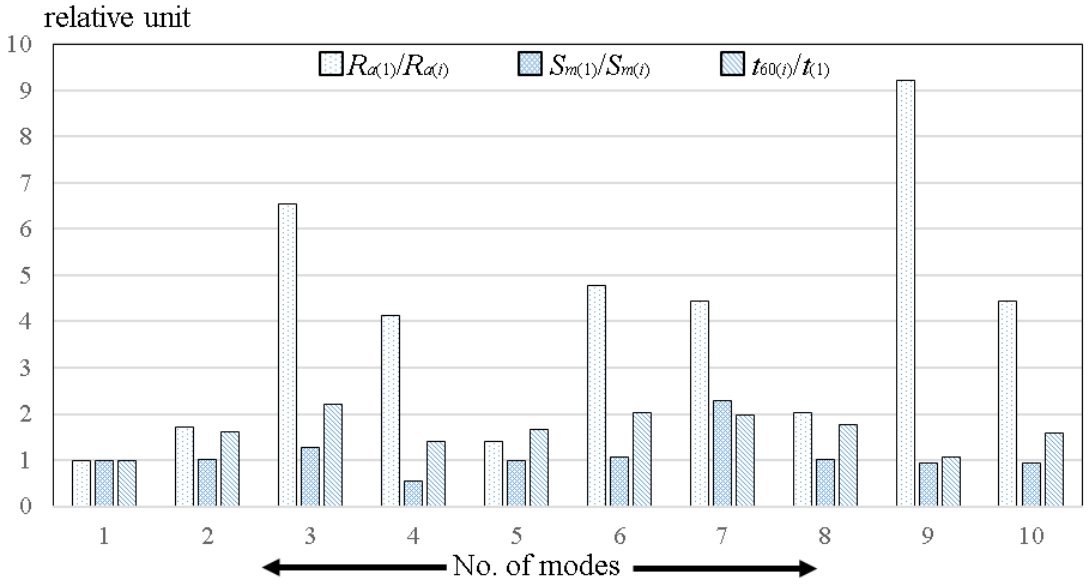

Fig. 5. Comparison of different processing modes (1–10) for three types of roughness parameters (R_a, S_m, t_{60})

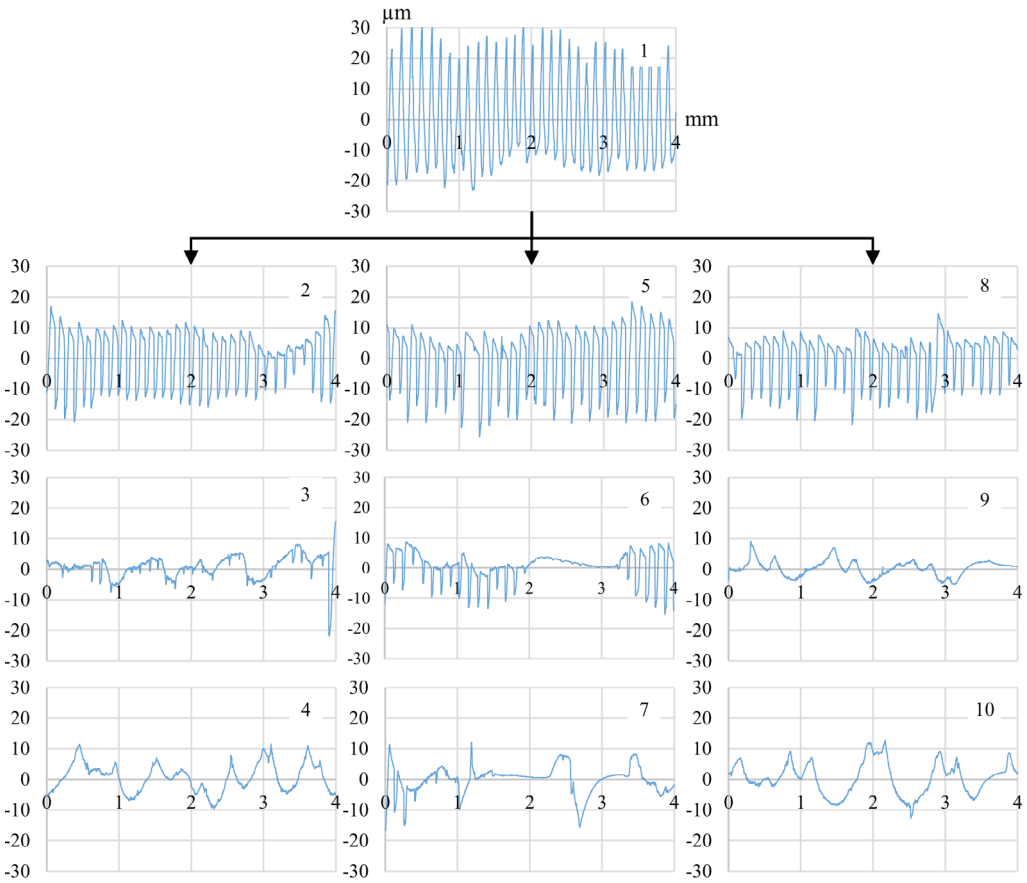

Fig. 6. The surface layer profilograms of titanium alloy after different processing modes (1–10)

Profilogram analysis (Fig. 6) indicated that *AC*-based processing promotes pronounced waviness and a high-rigidity profile (Fig. 6, **Mode 10**). *DC* causes greater heating of the initial micro-protrusions from turning, reducing their deformation resistance and minimizing vibration during smoothing (Fig. 6, **Mode 7**) [8]. *EMP* with *DC* of 300 A/mm² showed partial technological inheritance of the semi-finish turning profile (Fig. 6, **Mode 6**).

Profiles from **Modes 4** and **7**, despite their concave shape and lower rigidity, and load-bearing capacity, possess adequate oil retention and can be suitable for specific friction pair applications [7, 8].

Applying the fast Fourier transform (*FFT*) yielded characteristic profilograms representing the main amplitude-frequency components of the discrete signal, excluding subharmonic "noise" (Fig. 7, **Modes 1–10**).

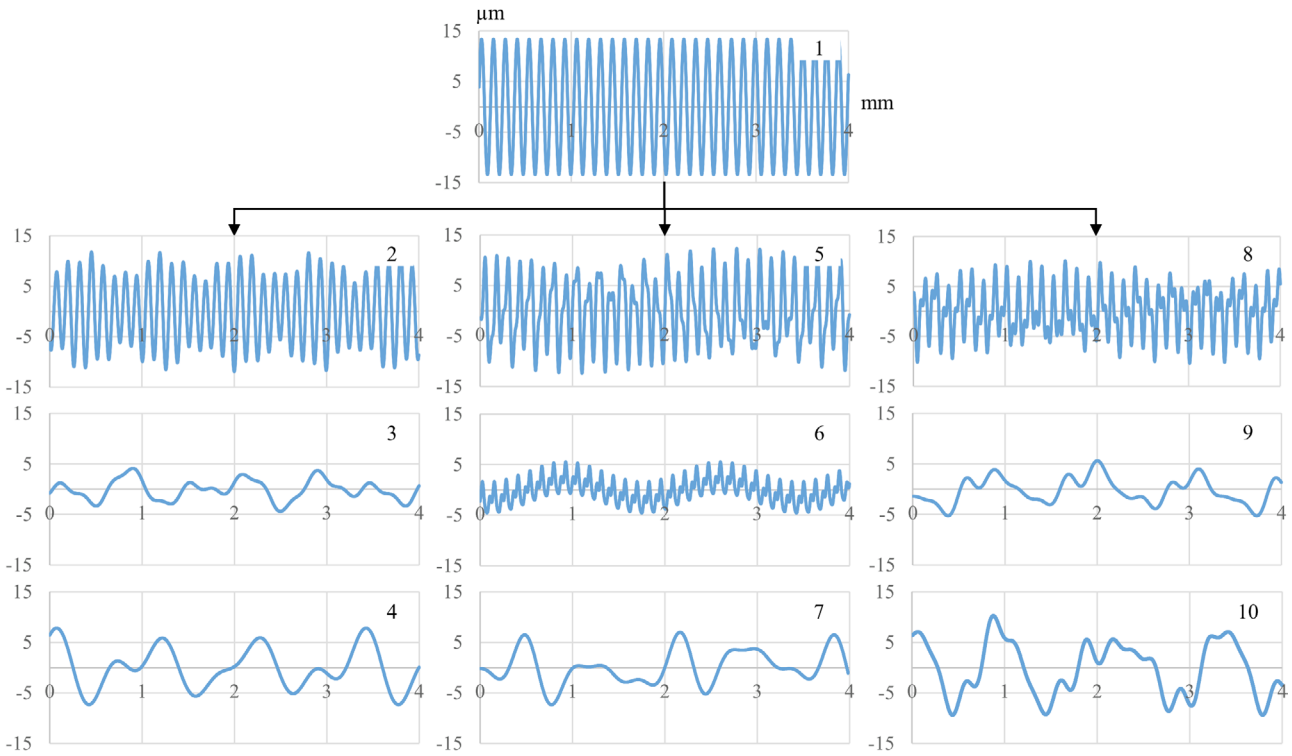

Fig. 7. The surface model profilograms of titanium alloy *VT22* after *FFT* by fundamental harmonics

For the initial state and modes involving simple running-in or low-current-density processing (100 A/mm²), the dominant harmonic corresponds to the semi-finish turning (Fig. 7, **Modes 1, 2, 5, 8**).

EMP with high current density (**Modes 3-4, 6-7, 9-10**) generated profiles with a prominent low-frequency component and smoother irregularities (reducing $\boldsymbol{R_a}$ by up to 9.2 times and $\boldsymbol{S_m}$ by 2.28 times). Fig. 7 shows that increasing current density during *EMP* suppresses high-frequency profile components, giving rise to a dominant ("carrier") frequency.

Fig. 8 presents the curves of relative bearing surfaces for different levels of ***P*** **Modes 1–10**. Based on these curves, microprofiles are classified as:

Low-rigidity: **Modes 1–6**

Medium-rigidity: **Modes 8** and **9**

High- rigidity: **Modes 7** and **10.**

For applications requiring reliable interference fits (resistant to premature loosening from asperity crushing) and low wear in friction pairs, *DC EMP* at 300 or 600 A/mm^2 – in either smoothing (10 N) or deformation (150 N) modes – is recommended. The improvement stems from increased actual contact area [26].

The strength of the interference fit and the tightness of the connections are achieved due to larger actual contact support areas [26].

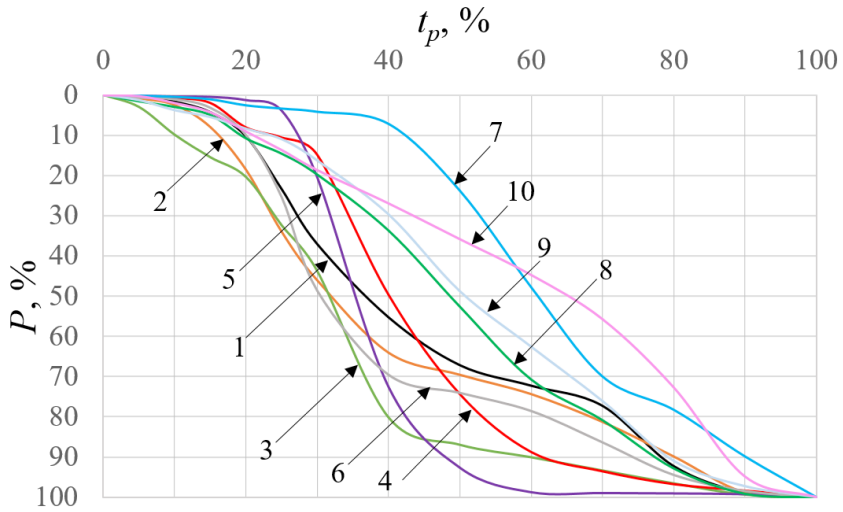

Fig. 8. Profile reference line curves for modes 1–10

For example, model surface profile curves for **Modes 2**, **4**, and **5** are decomposed into their constituent harmonics (Figs. 9, *a–f*).

As shown in Fig. 9, *d*, it is evident that despite the plastic deformation of the surface by the roller, the prevailing period remained the feed rate of the cutter during semi-finishing, i.e., 0.125 mm.

For *DC EMP* with a current density of 600 A/mm² (Fig. 9, *e,* Fig. 6, 9*,* **Mode 7**), the main harmonic shifts toward longer periods, indicating profile waviness. The large roller radius caused overlapping processing tracks, which broadened (blurred) the main peak in the spectrogram (Fig. 9, *e*). A similar effect is observed for **Mode 10** (Fig. 9, *f*), where a minimum of five harmonics were required to achieve a visually accurate fit to the original profilogram and the highest correlation coefficient (Fig. 9, *c*).

To classify the scale of longitudinal profile deviations for the model curves, the ratio of the step length to the height of the protrusion (***l***/***H***) was calculated for each mode and harmonic (Fig. 10).

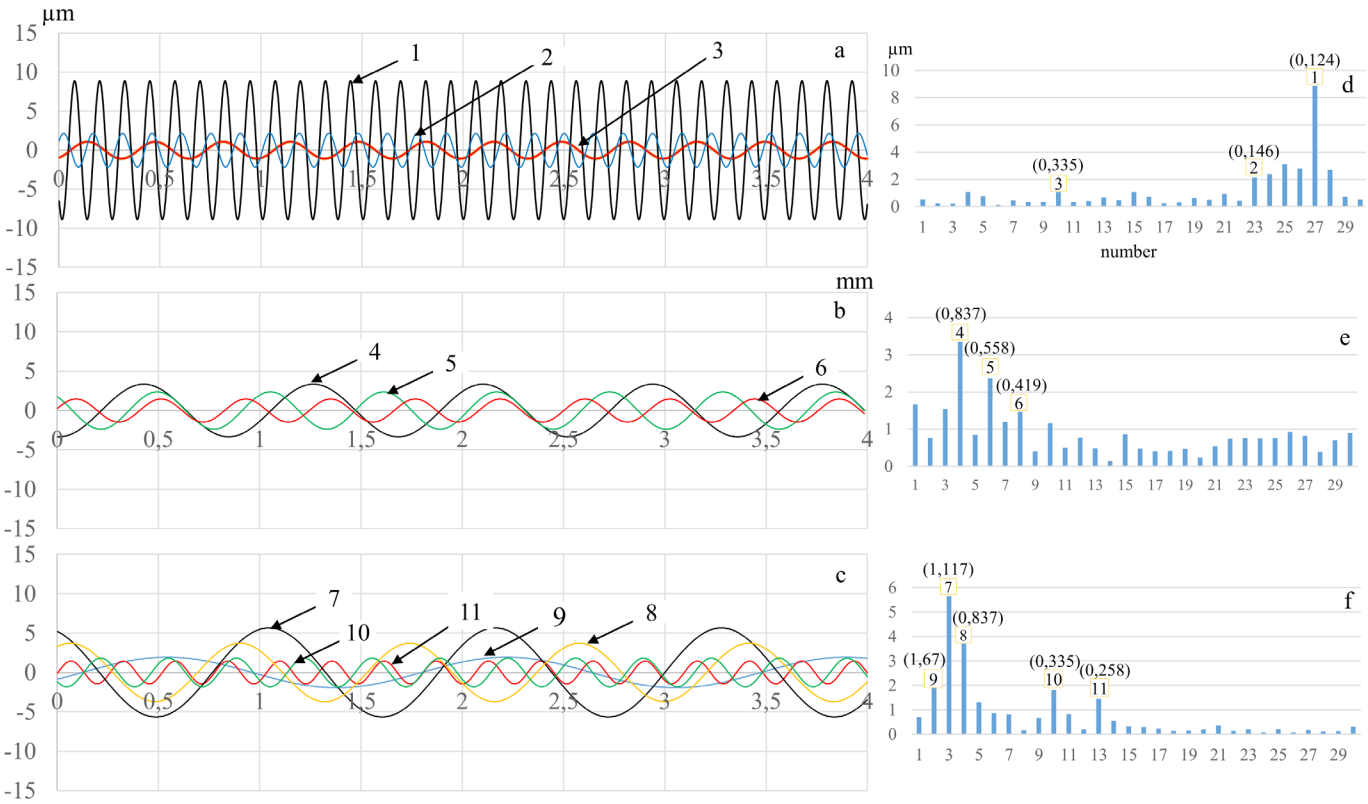

Fig. 9. Example of harmonic decomposition of model surface profile curves for modes 2, 7, and 10 (*a–c*). Numbers in *a–c* indicate harmonics (in order of decreasing amplitudes), *d–e* – spectrograms (periods are indicated in brackets)

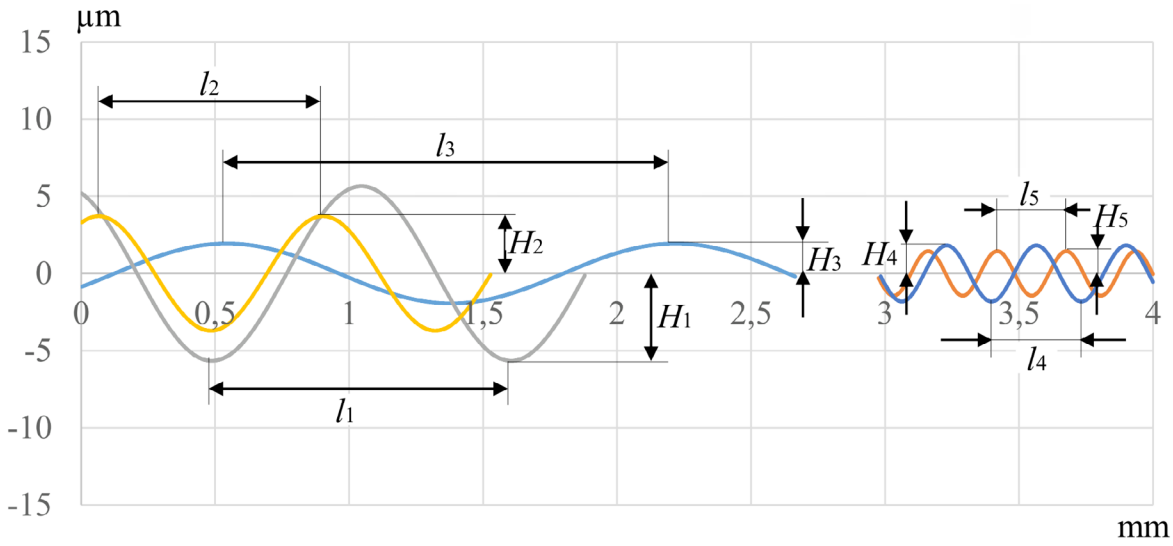

Fig. 10. Example of a diagram for determining the type of deviation of the longitudinal profile

Fig. 10 illustrates the determination of the ***l*/*H*** ratio and the corresponding deviation scale using five harmonics from **Mode 10** as an example.

The ***l*/*H*** ratios calculated for all processing modes of the *VT22* titanium alloy sample are presented in Fig. 11.

Harmonics corresponding to surface roughness are evident in **Modes 1**, **2**, **5**, **6**, and **8** (Fig. 11). These are inherited from the preceding semi-finish turning operation (0.125 mm/rev feed rate) and persist on the profilograms (Fig. 6) due to the weak thermomechanical impact of the working tool under these conditions. In contrast, these roughness-related harmonics are entirely absent in modes processed with higher current densities (**Modes 3**, **4**, **7**, **9**, and **10**), regardless of current type (Fig. 11). The lowest ***l*/*H*** ratios were recorded for **Modes 5** and **8**.

As noted in prior studies [7, 8, 28], surface engineering technologies such as vibro-rolling and electromechanical processing can create specific micro-reliefs designed to enhance lubrication. This is achieved by forming artificial micro-wedges between friction pairs, which can initiate a hydrodynamic lubrication effect. For instance, electromechanical processing was shown to increase the wear resistance of Steel 45 (0.45% *C*) and *VT22* titanium alloy by factors of 5 and 100, respectively, compared to their initial states. This significant improvement is attributed to the formation of oil-retaining pockets and a high-strength surface layer [29, 30].

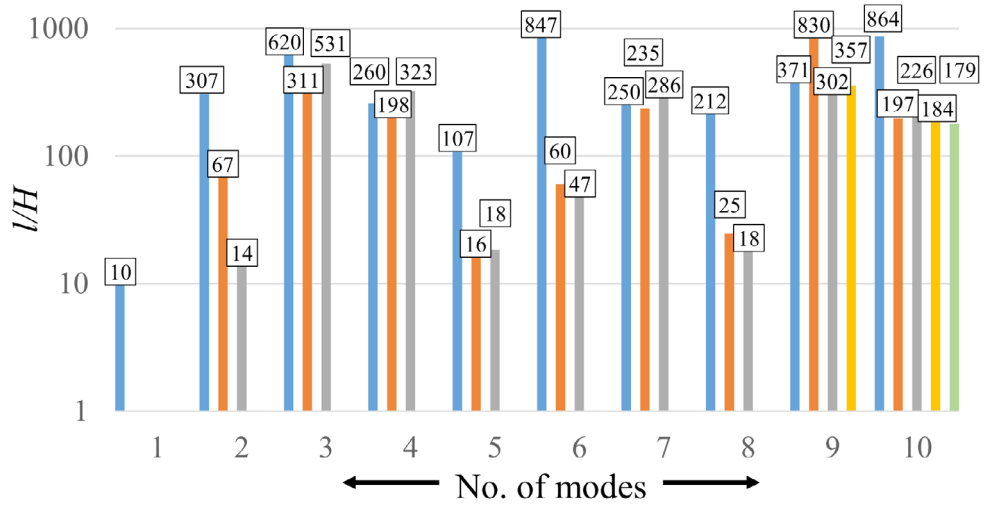

Fig. 11. Diagrams of the *l*/*H* ratio of modes 1–10 (the numbers above the columns are the *l*/*H* harmonic values). Note: the ordinate axis is given on a logarithmic scale

Analysis of the correlation coefficients (Table 2) reveals a strong correlation ($\boldsymbol{R} \geq 0.7$) for the surface layer hardened by roller tool processing (**Mode 2**) and for electromechanical smoothing/processing with alternating current (**Modes 4** and **9**). A moderate correlation ($0.5 \leq \boldsymbol{R} \leq 0.7$) is observed for **Modes 1** and **3**.

Table 2

Correlation coefficients between experimental data and model profile curves

Mode No.	1	2	3	4	5	6	7	8	9	10
Correlation coefficient $\|R\|$	0.57	0.71	0.51	0.73	0.20	0.23	0.37	0.26	0.74	0.40

In contrast, a weak correlation between the model curves and experimental data is found for *EMP* using direct current with a 150 N force at densities of 100, 300, and 600 A/mm² (**Modes 5**, **6**, **7**), as well as for alternating current *EMP* at 100 and 600 A/mm² with the same force (**Modes 8** and **10**).

The low correlation coefficient for **Mode 5** may result from spectral amplitudes falling into adjacent frequencies, which can distort or mask lower-amplitude peaks [31]. The authors attribute the small ***R***-value for **Mode 6** to the absence of a distinct cyclic component over more than one-third of the profile length, indicating the limited sensitivity of this mathematical approach to localized signal variations.

Optimum interference fits for movable joints require surfaces with low height parameters. High-profile asperities promote premature loosening and wear via plastic deformation, compromising joint sealing and accelerating corrosion [32]. Furthermore, increasing the bearing length ratio ($\boldsymbol{t_p}$) and mean spacing of profile irregularities ($\boldsymbol{S_m}$) reduces the friction coefficient and enhances wear resistance. A high $\boldsymbol{S_m}$ combined with a low $\boldsymbol{R_a}$ significantly mitigates the stress-concentrating effect of surface irregularities, thereby improving fatigue strength and durability [33].

Proper selection of *EMP* and *SPD* modes, coupled with precise process control and analytical techniques like *FFT*, enables the production of high-quality surface profiles. This approach minimizes artifacts from sample vibration, fluctuating contact pressure against the current collector, and other experimental variabilities.

Conclusion

1. Analysis of surface profilograms for the *VT22* titanium alloy demonstrated that all applied processing modes reduced height parameters (achieving $\boldsymbol{R_a}$ as low as 1.35 μm) and improved the surface finish grade from 3 to 6. Electromechanical processing (*EMP*) with high-density direct current was particularly effective in qualitatively suppressing profile "chatter" inherited from the preceding semi-finish turning.

2. Electromechanical processing and smoothing (**Modes 3, 6, 7**) significantly reduce the profile step parameter by up to a factor of 2.28 and increase the relative bearing length to 98.8%, producing "oil-pockets" profiles with varying rigidity levels and waviness characterized by different step and height parameters.

3. The application of the fast *Fourier* transform (*FFT*) enabled the identification of principal components resulting from the complex multi-stage processing, isolation of the profile's cyclic component, generation of profile irregularity distribution graphs based on approximation models, and filtering of random artifacts from the process (e.g., potential vibration, low system rigidity, and sample flapping in the chuck) for correct interpretation of the results obtained. The highest correlation coefficient ($\boldsymbol{R} > 0.7$) was observed for surface plastic deformation (*SPD*) and alternating current electromechanical processing (*EMP*), attributable to the combined dominance of the trend from the preceding semi-finish turning and the waviness induced by *EMP* (**Modes 2**, **4**, **9**).

4. Fast *Fourier* transform (*FFT*) can be used as an express assessment and classification by the scale factor of longitudinal deviations of the machine parts' surface profile after various types of processing.

5. As the most optimal processing mode in terms of surface microgeometry parameters for a mechanical engineering technologist, **Mode 3** is recommended. It effectively reduces height and step parameters and significantly increases the structural parameter responsible for the load-bearing capacity of mating parts.

References

1. Heifetz M.L., Gretsky N.L., Prement G.B. Technological inheritance of operational quality parameters in the life cycle of internal combustion engine parts. *Naukoemkie tekhnologii v mashinostroenii = Science Intensive Technologies in Mechanical Engineering*, 2019, no. 7 (97), pp. 35–42. DOI: 10.30987/article_5cf7bd2fec77a9.13115279. (In Russian).

2. Averchenkov V.I., Vasiliev A.S., Heifetz M.L. Technological heredity in the formation of the quality of manufactured parts. *Naukoemkie tekhnologii v mashinostroenii = Science Intensive Technologies in Mechanical Engineering*, 2018, no. 10 (88), pp. 27–32. (In Russian).

3. Grzesik W., Żak K., Chudy R., Prażmowski M., Małecka J. Optimization of subtractive-transformative hybrid processes supported by the technological heredity concept. *CIRP Annals*, 2019, vol. 68 (1), pp. 101–104. DOI: 10.1016/j.cirp.2019.03.005.

4. Fedorov A.A., Zhdanova Yu.E., Linovskii A.V., Bobkov N.V., Bredgauer Yu.O. Vliyanie fazovogo sostava titanovykh splavov na parametry sherokhovatosti, poluchaemye v protsesse provolochnoi elektroerozionnoi obrabotki [Influence of the phase composition of titanium alloys on the roughness parameters obtained during wire electrical discharge machining]. *Omskii nauchnyi vestnik = Omsk Scientific Bulletin*, 2021, no. 4 (178), pp. 18–24. DOI: 10.25206/1813-8225-2021-178-18-24. (In Russian).

5. Muratkin G.V., Sarafanova V.A. Vliyanie tekhnologicheskoi nasledstvennosti napryazhenno-deformirovannogo sostoyaniya na tochnost' nezhestkikh detalei [Influence of technological heredity of the stress-strain state on the accuracy of non-rigid parts]. *Problemy mashinostroeniya i nadezhnosti mashin = Problems of Mechanical Engineering and Machine Reliability*, 2020, no. 1, pp. 56–64. DOI: 10.31857/S0235711920010095.

6. Zhang H., Ren Z., Liu J., Zhao J., Liu Z., Lin D., Zhang R., Graber M.J., Thomas N.K., Kerek Z. D., Wang G.-X., Dong Y., Ye C. Microstructure evolution and electroplasticity in Ti64 subjected to electropulsing-assisted laser shock peening. *Journal of Alloys and Compounds*, 2019, vol. 802, pp. 573–582. DOI: 10.1016/j.jallcom.2019.06.156.

7. Bagmutov V.P., Parshev S.N., Dudkina N.G., Zakharov I.N., Savkin A.N., Denisevich D.S. *Elektromekhanicheskoe uprochnenie metallov i splavov* [Electromechanical hardening of metals and alloys]. Volgograd, VolgSTU Publ., 2016. 460 p.

8. Askinazi B.M. *Uprochnenie i vosstanovlenie detalei mashin elektromekhanicheskoi obrabotkoi* [Strengthening and restoration of machine parts by electromechanical treatment]. 3rd ed., rev. Moscow, Mashinostroenie Publ., 1989. 200 p.

9. Sneddon S., Xu Y., Dixon M., Rugg D., Li P., Mulvihill D.M. Sensitivity of material failure to surface roughness: A study on titanium alloys Ti64 and Ti407. *Materials & Design*, 2021, vol. 200, p. 109438. DOI: 10.1016/j.matdes.2020.109438.

10. Gao K., Zhang Y., Yi J., Dong F., Chen P. Overview of surface modification techniques for titanium alloys in modern material science: A comprehensive analysis. *Coatings*, 2024, vol. 14 (1), p. 148. DOI: 10.3390/coatings14010148.

11. Ojo S.A., Manigandan K., Morscher G.N., Gyekenyesi A.L. Enhancement of the microstructure and fatigue crack growth performance of additive manufactured titanium alloy parts by laser-assisted ultrasonic vibration processing. *Journal of Materials Engineering and Performance*, 2024, vol. 33, pp. 10345–10359. DOI: 10.1007/s11665-024-09323-8.

12. Amanov A., Yeo I.K., Jeong S.H. Advanced post-processing of Ti6Al4V alloy fabricated by selective laser melting: A study of laser shock peening and ultrasonic nanocrystal surface modification. *Journal of Materials Research and Technology*, 2025, vol. 35, pp. 4020–4031. DOI: 10.1016/j.jmrt.2025.02.038.

13. Liu R., Yuan S., Lin N., Zeng Q., Wang Z., Wu Y. Application of ultrasonic nanocrystal surface modification (UNSM) technique for surface strengthening of titanium and titanium alloys: A mini review. *Journal of Materials Research and Technology*, 2021, vol. 11, pp. 351–377. DOI: 10.1016/j.jmrt.2021.01.013.

14. Nakatani M., Masuo H., Tanaka Y., Murakami Y. Effect of surface roughness on fatigue strength of Ti-6Al-4V alloy manufactured by additive manufacturing. *Procedia Structural Integrity*, 2019, vol. 19, pp. 294–301. DOI: 10.1016/j.prostr.2019.12.032.

15. Civiero R., Perez-Rafols F., Nicola L. Modeling contact deformation of bare and coated rough metal bodies. *Mechanics of Materials*, 2023, vol. 179, p. 104583. DOI: 10.1016/j.mechmat.2023.104583.

16. Han T., Fan J. Ultrasonic measurement of contact stress at metal-to-metal interface based on a real rough profile through modeling and experiment. *Measurement*, 2023, vol. 217, p. 113046. DOI: 10.1016/j.measurement.2023.113046.

17. Qi B., Huang X., Guo W., Ren X., Chen H., Chen X. A novel comprehensive framework for surface roughness prediction of integrated robotic belt grinding and burnishing of Inconel 718. *Tribology International*, 2024, vol. 195, p. 109574. DOI: 10.1016/j.triboint.2024.109574.

18. Xue Z., Lai M., Xu F., Fang F. Influence factors and prediction model of surface roughness in single-point diamond turning of polycrystalline soft metal. *Journal of Materials Processing Technology*, 2024, vol. 324, p. 118256. DOI: 10.1016/j.jmatprotec.2023.118256.

19. Stampfer B., Bachmann J., Gauder D., Böttger D., Gerstenmeyer M., Lanza G., Wolter B., Schulze V. Modeling of surface hardening and roughness induced by turning AISI 4140 QT under different machining conditions. *Procedia CIRP*, 2022, vol. 108, pp. 293–298. DOI: 10.1016/j.procir.2022.03.050.

20. Li S., Li S., Liu Z., Petrov A.V. Roughness prediction model of milling noise-vibration-surface texture multidimensional feature fusion for N6 nickel metal. *Journal of Manufacturing Processes*, 2022, vol. 79, pp. 166–176. DOI: 10.1016/j.jmapro.2022.04.055.

21. Sakthivel N.R., Cherian J., Nair B.B., Sahasransu A., Aratipamula L.N.V.P., Gupta S.A. An acoustic dataset for surface roughness estimation in milling process. *Data in Brief*, 2024, vol. 57, p. 111108. DOI: 10.1016/j.dib.2024.111108.

22. Wang J., Wu X., Huang Q., Mu Q., Yang W., Yang H., Li Z. Surface roughness prediction based on fusion of dynamic-static data. *Measurement*, 2025, vol. 243, p. 116351. DOI: 10.1016/j.measurement.2024.116351.

23. Bagmutov V.P., Vodopyanov V.I., Zakharov I.N., Ivannikov A.Y., Bogdanov A.I., Romanenko M.D., Barinov V.V. Features of changes in the surface structure and phase composition of the of α + β titanium alloy after electromechanical and thermal treatment. *Metals*, 2022, vol. 12 (9), p. 1535. DOI: 10.3390/met12091535.

24. He J., Li B., Sun Q., Li Y., Lyu H., Wang W., Xie Z. The improved fault location method based on natural frequency in MMC-HVDC grid by combining FFT and MUSIC algorithms. *International Journal of Electrical Power & Energy Systems*, 2022, vol. 137, p. 107816. DOI: 10.1016/j.ijepes.2021.107816.

25. Fedorov V.L. Kriterii opredeleniya chisla garmonik ryadov Fur'e, approksimiruyushchikh napryazheniya i toki transformatora [Criterion for determining the number of harmonics of Fourier series approximating transformer voltages and currents]. *Omskii nauchnyi vestnik = Omsk Scientific Bulletin*, 2018, no. 5 (161), pp. 82–89. DOI: 10.25206/1813-8225-2018-161-82-89.

26. Muratkin G.V., comp. *Konspekt lektsii po distsipline «Osnovy vosstanovleniya detalei i remont avtomobilei»* [Lecture notes on the discipline "Fundamentals of Parts Restoration and Car Repair"]. Tolyatti, TSU Publ., 2008. 120 p.

27. Malyshko S.B., Tarasov V.V. [The influence of the technological parameters of the electromechanical treatment on the surface roughness]. *Problemy transporta Dal'nego Vostoka* [Problems of Transport in the Far East]. Proceedings from 13th Scientific and Practical Conference. Vladivostok, 2019, pp. 63–65. (In Russian).

28. Uchkin P.G. Primenenie vibronakatyvaniya gil'z tsilindrov dvigatelya vnutrennego sgoraniya s tsel'yu uvelicheniya ikh resursa [The use of vibration rolling of cylinder liners of an internal combustion engine in order to increase their resource]. *Izvestiya Orenburgskogo gosudarstvennogo agrarnogo universiteta = Izvestia Orenburg State Agrarian University*, 2023, no. 2 (100), pp. 99–105. DOI: 10.37670/2073-0853-2023-100-2-99-105.

29. Parshev S.N., Serov I.M., Zubkov A.V., Korobov A.V. Vliyanie impul'snogo elektromekhanicheskogo uprochneniya na iznosostoikost' podvizhnykh sopryazhenii [Influence of pulsed electromechanical hardening on the wear resistance of movable joints]. *Molodoi uchenyi = Young Scientist*, 2015, no. 23 (103), pt. 2, pp. 200–204.

30. Bagmutov V.P., Zakharov I.N., Romanenko M.D., Barinov V.V., Tikhaeva V.V. Influence of technological modes of combined high-energy treatment on wear resistance of transition class titanium alloy. *Russian Physics Journal*, 2024, vol. 67 (10), pp. 1647–1653. DOI: 10.1007/s11182-024-03294-y.

31. Manus H. An ultra-precise fast Fourier transform. *Science Talks*, 2022, vol. 4, p. 100097. DOI: 10.1016/j.sctalk.2022.100097.

32. Leonov O.A., Vergazova Yu.G. Otnositel'naya opornaya dlina profilya poverkhnosti i dolgovechnost' detalei [Relative bearing length of the surface profile and durability of parts]. *Innovatsionnaya nauka = Innovative Science*, 2016, no. 1-2 (13), pp. 81–83.

33. Aliev A.A., Bulgakov V.P., Prikhod'ko B.S. Kachestvo poverkhnosti i svoistva detalei mashin [Surface quality and properties of machine parts]. *Vestnik Astrakhanskogo gosudarstvennogo tekhnicheskogo universiteta = Vestnik of Astrakhan State Technical University*, 2004, no. 1 (20), pp. 8–12.

Conflicts of Interest

The authors declare no conflict of interest.